†This work was supported by the U. S. Atomic Energy Commission, under Contract No. AT-(40-1)-3677.

*Present address: Naval Research Laboratory, Washington, D.C. 20390.

[1]J. S. Cook and J. S. Dryden, Australian J. Phys. 13, 260 (1960); Proc. Phys. Soc. (London) 80, 479 (1962).

[2]J. F. Symmons and R. C. Kemp, Brit. J. Appl. Phys. 17, 607 (1966).

[3]R. Cappelletti and E. DeBenedetti, Phys. Rev. 165, 981 (1968).

[4]J. Quin, B. A. W. Redfern, and P. L. Pratt, Proc. Brit. Ceram. Soc. 9, 35 (1967).

[5]A. B. Lidiard, in *Proceedings of the Bristol Conference on Defects in Crystalline Solids*, 1954 (The Physical Society, London, 1955), p. 283.

[6]R. W. Dreyfus, Phys. Rev. 121, 1675 (1961).

[7]C. Bucci and R. Fieschi, Phys. Rev. Letters 12, 16 (1964).

[8]G. D. Watkins, Phys. Rev. 113, 79 (1959).

[9]J. S. Dryden and G. S. Harvey, J. Phys. C 2, 643 (1969).

[10]W. C. Collins and J. H. Crawford, Solid State Commun. (to be published).

[11]J. H. Crawford, J. Phys. Chem. Solids 31, 399 (1970).

[12]H. J. Wintle, Phys. Rev. 179, 769 (1969).

[13]W. J. Fredericks (private communication).

PHYSICAL REVIEW B VOLUME 4, NUMBER 10 15 NOVEMBER 1971

Force-Constant Changes and the Crystal Impurity Problem

Philip D. Mannheim*
Université Libre de Bruxelles, Faculté des Sciences, Pool de Physique, Bruxelles, Belgium
and
Simon S. Cohen
Department of Chemistry, Technion-Israel Institute of Technology, Haifa, Israel
(Received 3 May 1971)

We study the crystal impurity problem for the case of nearest-neighbor force-constant changes around the defect site of body-centered and face-centered cubic crystals. We discuss general group-theoretical techniques for determining the dynamics of the system and also its response to an external optical probe. We provide closed-form expressions for all the necessary dynamical quantities, and show that their determination only requires knowledge of the pure-crystal density of states in cases where there are only central forces. We apply our results to the absorption spectra of xenon and of krypton in solid argon, to obtain good agreement with the observed data.

I. INTRODUCTION

This paper is a direct continuation of an analysis previously carried out by one of the authors.[1] Some of the results presented in this work have already been provided in Ref. 1, and we present them here only so that this paper may be self-contained. As well as providing some new results on the response of an impure system to an optical probe, we have also found what we regard as simpler derivations of some of the results of Ref. 1. The literature on the crystal impurity problem is expanding at an enormous rate and we suspect that some of our observations have already been reported, though unknown to us. We refer the reader to Ref. 2 and references cited in Refs. 1 and 2 for a more comprehensive review of the field. The notation we use throughout is the same as given in Ref. 1.

For studies of the lattice dynamics of both pure and impure crystal systems the three essential theoretical quantities are $\nu(\omega)$, $|\chi^2(l, \omega^2)|$, and $K(\omega)$. $\nu(\omega)$ is the density of states at a frequency ω. $|\chi^2(l, \omega^2)|$ is the amplitude of vibration of the atom at site l in the lattice mode of frequency ω, and $K(\omega)$ is the linear-response function of the system to an external probe. The physical observables of experiments such as optical absorption, Mössbauer effect, and neutron scattering may be expressed in terms of these quantities, and hence their determination is paramount. In the impure system in particular these quantities show radical departures from their pure-crystal values, and since we have added a source term to the pure-crystal equations of motion, we may solve for them using the lattice-Green's-function technique.

All of the qualitative features of the problem, such as the presence and properties of localized and resonance modes, were established by a study of the isotopic impurity.[2,3] Using group-theoretical techniques which exploit the high (O_h) symmetry at the defect site,[2,4] it is possible to extend the analysis to incorporate force-constant changes as well. Though conceptually the extension is direct, in practice the work is laborious as there are a large number of degrees of freedom (the coordinates of the atoms in the near-neighbor cluster), and hence a large number of lattice Green's functions are required. Since the defect displacement transforms

like a vector it only contributes to the F_{1u}-mode representations of O_h. These appear three times for the bcc crystal and four times for the fcc crystal in the total representations of the respective clusters. (These are 27 dimensional for the bcc crystal and 39 dimensional for the fcc crystal.) Thus symmetry allows a block diagonalization of the relevant Green's-function matrices and reduces the problem to treating three- or four-dimensional matrices. These have been handled numerically with approximations in certain cases,[5,6] where it is then difficult to keep track of what is going on.

In Ref. 1 we observed that the lattice Green's functions are also constrained by the O_h symmetry, and we obtained relations among them. This then enabled us to find closed analytic expressions for $\nu(\omega)$ and $|\chi^2(0,\omega^2)|$ and determine the positions of the localized and resonance modes for the case of nearest-neighbor central force changes in bcc and fcc crystals. In this work we again determine $|\chi^2(0,\omega^2)|$ by a slightly simpler method, and also find a closed-form expression for $K(\omega)$ under the same assumptions. The relation we obtain is remarkably simple, and as before only requires knowledge of the pure-crystal density of states and the force-constant ratio. For convenience we assemble here our results which obtain in both the bcc and fcc cases. We introduce M and $A_{xx}(00)$ as the mass and force constant at the defect site, respectively, and use primes to denote the changed values. We define

$$\lambda = 1 - A'_{xx}(00)/A_{xx}(00), \quad \epsilon = 1 - M'/M, \tag{1}$$

$$\rho(\omega^2) = \epsilon/(1-\epsilon) - 2\,\omega^2/\omega^2_{\max}\,[\lambda/(1-\lambda)], \tag{2}$$

$$S(\omega^2) = P\int \omega'^2\,\nu(\omega'^2)/(\omega^2-\omega'^2)\,d\omega'^2, \tag{3}$$

$$T(\omega^2) = \omega^4 \int \nu(\omega'^2)/(\omega^2-\omega'^2)^2\,d\omega'^2\,. \tag{4}$$

Here $\nu(\omega^2) = \nu(\omega)/2\omega$ is the density of squared states in the pure crystal, and we have introduced the usually experimentally known maximum frequency through the relation[1,7]

$$\omega^2_{\max} = 2A_{xx}(00)/M. \tag{5}$$

The condition for resonance and localized modes is[1]

$$1 - \rho(\omega^2)\,S(\omega^2) = 0 \tag{6}$$

and the amplitude of vibration of the defect is[1]

$$|\chi^2(0,\omega^2)| = \sum_\alpha |\chi^2_\alpha(0,\omega^2)|$$

$$= \frac{1}{MN}\left(\frac{M}{M'}\right)^2 \{[1-\rho(\omega^2)S(\omega^2)]^2 + [\pi\omega^2\nu(\omega^2)\rho(\omega^2)]^2\}^{-1} \tag{7a}$$

or

$$= \frac{1}{M}\left(\frac{M}{M'}\right)^2 \left(\rho^2(\omega_L^2)T(\omega_L^2) + \frac{M}{M'} - [1+\rho(\omega_L^2)]^2\right)^{-1}, \tag{7b}$$

where Eq. (7a) is valid for band modes and Eq. (7b) is obtained in the event of a localized mode. In Refs. 1 and 8 we also give expressions for the change in the density of states for any ω and for the defect mean-square velocity and mean-square displacement.

In this work we find the relation

$$K(\omega) \sim \tfrac{1}{2}\pi N\,(\omega/\omega_{\text{cell}})^4\,|\chi^2(0,\omega^2)|\;\nu(\omega) \tag{8}$$

up to a frequency-independent factor which depends on the nature of the probe. Here we have introduced

$$\omega^2_{\text{cell}} = A'_{xx}(00)/M', \tag{9}$$

the cell frequency of the defect moving in an oscillator potential provided by the neighbors, i.e., a particle in a box. We shall discuss the physics of this cell-model limit below. Equation (8) is not just the response of the defect but is the response of the *whole* F_{1u} mode, and includes those motions of the neighbors which contribute to the mode as well.

We have not studied the most general case of noncentral forces as well, but we suspect the results will continue to hold apart from suitable changes in $\rho(\omega^2)$. We hope to examine this point further in a future publication. The plan of this paper is to present first the general method, and then the calculation in the specific cases of interest. We conclude with an application to the far-ir absorption spectra of xenon and krypton impurities in solid argon, and with a general discussion of our work.

II. GENERAL METHOD

In the harmonic approximation the equations of motion of a $3N$-dimensional crystal lattice are given by

$$\sum_{\beta,l'} [A_{\alpha\beta}(l,l') - \omega^2 M(l')\delta_{\alpha\beta}\delta(l,l')]u_\beta(l') = 0, \tag{10}$$

where $\alpha = x, y, z$ for monatomic lattices and l goes from 1 to N. Here $A_{\alpha\beta}(l,l')$ are the second-order force constants, and the displacement from equilibrium of the atom at site $\vec{R}(l)$ is given by $e^{i\omega t}\vec{u}(l)$. It is convenient to introduce the dynamical matrix[9]

$$D_{\alpha\beta}(\vec{K}) = (1/M)\textstyle\sum_l A_{\alpha\beta}(0,l)e^{-i\vec{K}\cdot\vec{R}(l)}, \tag{11}$$

whose eigenvectors and eigenvalues satisfy

$$\textstyle\sum_\beta D_{\alpha\beta}(\vec{K})\sigma^j_\beta(\vec{K}) = \omega^2_j(\vec{K})\,\sigma^j_\alpha(\vec{K}) \tag{12}$$

and also to introduce the pure lattice Green's functions

$$g_{\alpha\beta}(\omega;l,l') = \frac{1}{NM}\sum_{\vec{K},j}\frac{\sigma^{*j}_\alpha(\vec{K})\sigma^j_\beta(\vec{K})}{\omega^2_j(\vec{K})-\omega^2} \times \exp\{i\vec{K}\cdot[\vec{R}(l') - \vec{R}(l)]\}. \tag{13}$$

It is then easy to show that the Green's functions

satisfy

$$\sum_{\beta,l} A_{\alpha\beta}(0,l)\, g_{\alpha'\beta}(\omega; l, l') = \delta_{\alpha\alpha'} \frac{1}{N} \sum_{\vec{k}} e^{i\vec{k}\cdot\vec{R}(l')} + M\omega^2 g_{\alpha'\alpha}(\omega; 0, l'), \quad (14)$$

where we obtain the lattice Δ function $\Delta(\vec{R})$ on the right-hand side. Note that Eq. (14) is an exact result for all neighbor interactions and follows from the translational invariance of the lattice only. We shall find that Eq. (14) is crucial when we perform the calculations below. In Ref. 1 we calculated the necessary relations one at a time. Using this general relation they may be derived in a more direct manner.

We now introduce a point impurity substitutionally at the origin of coordinates. If we separate out the changes in mass and force constants as a perturbation

$$V_{\alpha\beta}(l, l') = -\omega^2(M - M')\delta_{\alpha\beta}\delta(l, 0)\delta(l', 0) + A_{\alpha\beta}(l, l') - A'_{\alpha\beta}(l, l'), \quad (15)$$

we may then rewrite Eq. (10) as

$$\sum_{\beta,l'} [A_{\alpha\beta}(l, l') - M\omega^2\delta_{\alpha\beta}\delta(l, l')]\, u_\beta(l') = \sum_{\beta,l'} V_{\alpha\beta}(l, l') u_\beta(l'). \quad (16)$$

We then solve Eq. (16) using the lattice-Green's-function technique. We only present the solution schematically. We write the Lippmann-Schwinger and Dyson equations as

$$\Psi = \Phi + G_0 V \Psi = (1 - G_0 V)^{-1}\, \Phi, \quad (17)$$

$$G = G_0 + G_0 V G = (1 - G_0 V)^{-1} G_0 . \quad (18)$$

We continue into the complex plane to give G_0 a real and imaginary part, i.e.,

$$G_0 = G_0^R + iG_0^I .$$

Then

$$|\Psi|^2 = |\Phi|^2 \{1/[(1 - G_0^R V)^2 + (G_0^I V)^2]\} ,$$
$$\mathrm{Im}G = 1/[(1 - G_0^R V)^2 + (G_0^I V)^2]\, G_0^I . \quad (19)$$

Thus

$$\mathrm{Im}G = |\Psi|^2\, [|\Phi|^2]^{-1}\, G_0^I . \quad (20)$$

We now return to the site representation after this somewhat cavalier derivation where we ignored questions of commutation of matrices, etc., where we have

$$\mathrm{Im}g_{\alpha\alpha}(\omega; 0, 0) = (\pi/M)\ \nu(\omega^2), \quad |\chi^2_{\mathrm{pure}}(0, \omega^2)| = 1/MN, \quad (21)$$

for the pure crystal, so that for the impure crystal we introduce $|\chi^2(0, \omega^2)|$ through a normal-mode expansion

$$u_\alpha(0) = (\hbar/2\omega)^{1/2} \sum_\omega \chi_\alpha(0, \omega^2)\, [a(\omega) + a^\dagger(\omega)],$$

and find

$$\mathrm{Im}G_{xx}(\omega; 0, 0) = \pi N\ \nu(\omega^2)\ |\chi^2(0, \omega^2)| . \quad (22)$$

Thus we may obtain the positions of the modes using the determinantal condition $|1 - G_0 V| = 0$, and may find $|\chi^2(0, \omega^2)|$ from Eq. (22). The major part of the calculation is then merely to determine and invert the matrix $1 - G_0 V$ in the F_{1u}-mode basis, and by use of Eq. (14) we are able to do this analytically. We are not aware that Eq. (22) has actually been used in the literature, though we presume it is known somewhere. Previously there were two other ways of obtaining $|\chi^2(0, \omega^2)|$. The authors of Ref. 3 appealed to the normalization condition

$$\sum_l M(l) |\chi^2(l, \omega^2)| = 1 \quad (23)$$

and proceeded to eliminate all $|\chi^2(l, \omega^2)|$ in favor of $|\chi^2(0, \omega^2)|$ using the equations of motion. Though easy enough for the isotopic case it is extraordinarily involved in the force-constant changes case, even using the symmetry, and has not been treated so far. In Ref. 1 we solved the problem by working with double-time Green's functions. This technique provides $\langle u_x^2(0)\rangle$ as an integral over the spectrum, and we were able to identify $|\chi^2(0, \omega^2)|$ as the integrand. Thus in that approach we in fact only determine $|\chi^2(0, \omega^2)|$ up to a function which may vanish on integrating. Also that was a quantum-mechanical derivation, and since we are dealing with oscillators we expect that there should be a classical solution. This is then given by Eq. (22) where we deal with $|\chi^2(0, \omega^2)|$ at each ω and not through an integral. It is reassuring to find that the results coincide. Equation (22) may also be generalized to find the amplitude of vibration of the neighbors in the perturbed modes, though we do not treat that here.

Finally the response function is given by[5,6,10]

$$K(\omega) = \omega\ \mathrm{Im}\ \mathrm{Tr}GQ, \quad (24)$$

where Q is the perturbation due to the external probe and the trace is taken over the requisite representation. [We note that in fact Eq. (22) is a special case of Eq. (24).] Thus our aim below is to solve Eqs. (22) and (24) using the symmetry method.

III. CALCULATION FOR BODY-CENTERED CUBIC LATTICE

The normalized threefold basis of the F_{1u} mode is given for the bcc lattice as[11]

$$\alpha_0 = u_x(0, 0, 0),$$
$$2\sqrt{2}\alpha_1 = u_x(1, 1, 1) + u_x(\bar{1}, 1, 1) + u_x(\bar{1}, \bar{1}, 1) + u_x(1, \bar{1}, 1) + u_x(\bar{1}, \bar{1}, \bar{1}) + u_x(1, \bar{1}, \bar{1}) + u_x(1, 1, \bar{1}) + u_x(\bar{1}, 1, \bar{1}),$$

$$
\begin{aligned}
4\alpha_2 = {} & u_y(1,1,1) + u_z(1,1,1) - u_y(\bar{1},1,1) - u_z(\bar{1},1,1) \\
& + u_y(\bar{1},\bar{1},1) - u_z(\bar{1},\bar{1},1) - u_y(1,\bar{1},1) + u_z(1,\bar{1},1) \\
& + u_y(\bar{1},\bar{1},\bar{1}) + u_z(\bar{1},\bar{1},\bar{1}) - u_y(1,\bar{1},\bar{1}) - u_z(1,\bar{1},\bar{1}) \\
& + u_y(1,1,\bar{1}) - u_z(1,1,\bar{1}) - u_y(\bar{1},1,\bar{1}) + u_z(\bar{1},1,\bar{1}).
\end{aligned} \tag{25}
$$

We introduce as in Ref. 1,

$$
\begin{aligned}
& g_0 = g_{xx}(000), \quad g_1 = g_{xx}(111), \quad g_2 = g_{xy}(111), \\
& Q = g_0 + g_{xx}(222) + g_{xx}(200) + g_{xx}(022) \\
& \qquad + 2g_{xx}(220) + 2g_{xx}(020), \\
& R = g_{xy}(222) + g_{xy}(220), \\
& S = g_0 + g_{yy}(222) - g_{yy}(020) - g_{yy}(202), \\
& T = g_{yz}(222) - g_{yz}(022),
\end{aligned} \tag{26}
$$

correcting some typing errors in Ref. 1 on the way. Thus in the normalized basis $(\alpha_0, \alpha_1, \alpha_2)$ the matrix of G_0 is

$$
[G_0]_{F_{1u}} = \begin{pmatrix} g_0 & 2\sqrt{2}g_1 & 4g_2 \\ 2\sqrt{2}g_1 & Q & \sqrt{2}R \\ 4g_2 & \sqrt{2}R & S+T \end{pmatrix} \tag{27}
$$

and the matrix of V is

$$
[V]_{F_{1u}} = \begin{pmatrix} V_{xx}(00) & 2\sqrt{2}V_{xx}(111) & 4V_{xy}(111) \\ 2\sqrt{2}V_{xx}(111) & -V_{xx}(111) & -\sqrt{2}V_{xy}(111) \\ 4V_{xy}(111) & -\sqrt{2}V_{xy}(111) & -V_{xx}(111) - V_{xy}(111) \end{pmatrix}, \tag{28}
$$

where we use $V_{\alpha\beta}(111)$ to denote $V_{\alpha\beta}(111, 0)$. We calculate the Green's-function relations from Eq. (14) and they can almost be read off from Eqs. (27) and (28). Assuming only nearest-neighbor forces they are

$$
\begin{aligned}
& A_{xx}(00)g_0 + 8A_{xx}(111)g_1 + 16A_{xy}(111)g_2 = 1 + M\omega^2 g_0, \\
& A_{xx}(00)g_1 + A_{xx}(111)Q + 2A_{xy}(111)R = M\omega^2 g_1, \\
& A_{xx}(00)g_2 + A_{xx}(111)R + A_{xy}(111)(S+T) = M\omega^2 g_2.
\end{aligned} \tag{29}
$$

We make the central-force approximation as previously,

$$
\begin{aligned}
& 8V_{xx}(111) = 8V_{xy}(111) = -\epsilon M\omega^2 - V_{xx}(00), \\
& 8A_{xx}(111) = 8A_{xy}(111) = -A_{xx}(00),
\end{aligned} \tag{30}
$$

so that Eqs. (27)–(29) may be reduced to the parameters M, $A_{xx}(00)$, ϵ, λ, and g_0. The determinant $|1 - G_0V|$ is now given by

$$
\Delta = (1-\lambda)(1-\epsilon)\,[1 - \rho(\omega^2)S(\omega^2)] \tag{31}
$$

so that $\Delta = 0$ gives Eq. (6). We next invert the matrix $1 - G_0V$ to obtain

$$
\Delta(1 - G_0V)^{-1} = \begin{pmatrix} 1 + \lambda M\omega^2(g_1 + 2g_2), & -\frac{1}{2\sqrt{2}}\lambda(1 + M\omega^2 g_0), & -\tfrac{1}{2}\lambda(1 + M\omega^2 g_0) \\ -2\sqrt{2}\,M\omega^2(\epsilon - \lambda)g_1, & 1 - \lambda + 2\lambda M\omega^2(1-\epsilon)g_2, \\ & \quad + M\omega^2(\epsilon - \lambda)g_0 & -\sqrt{2}\,\lambda M\omega^2(1-\epsilon)g_1 \\ -4M\omega^2(\epsilon - \lambda)g_2, & -\sqrt{2}\lambda M\omega^2(1-\epsilon)g_2 & 1 - \lambda + \lambda M\omega^2(1-\epsilon)g_1 \\ & & \quad + M\omega^2(\epsilon - \lambda)g_0 \end{pmatrix}, \tag{32}
$$

so that

$$
G_{xx}(\omega; 0, 0) = \frac{1 + S(\omega^2)\,[1 - \rho(\omega^2) + \epsilon/(1-\epsilon)]}{M\omega^2(1-\epsilon)\,[1 - \rho(\omega^2)S(\omega^2)]}. \tag{33}
$$

It is of course understood that in the above equation we are referring to the complex function $S(\omega^2 + i\epsilon)$, and not just the real part given in Eq. (3). Thus using Eq. (22) we obtain Eq. (7).

For the response of the system to an external probe, we note that the light must see the same symmetry as the defect sees. In the case that the absorption is due to induced dipole moments due to the polarization of the neighboring atoms by the defect atom, Q must have the same symmetry as that part of V which is due to changes in the electrostatic force constants. Thus for central forces,

$$
Q = \frac{\alpha^2}{8}\begin{pmatrix} 8 & -2\sqrt{2} & -4 \\ -2\sqrt{2} & 1 & \sqrt{2} \\ -4 & \sqrt{2} & 2 \end{pmatrix}, \tag{34}
$$

where the scale of Q is fixed by the effective charge α^2. From this it follows that

$$\mathrm{Tr}GQ = \frac{\alpha^2\{1 - S(\omega^2)\,[2\omega^2/\omega_{\max}^2 + \epsilon/(1-\epsilon)]\}}{A_{xx}(00)[1-\lambda][1-\rho(\omega^2)S(\omega^2)]} \quad (35)$$

so that

$$\omega\ \mathrm{Im}\ \mathrm{Tr}GQ = \alpha^2 \tfrac{1}{2}\pi N\ (\omega/\omega_{\mathrm{cell}})^4\ |\chi^2(0,\omega^2)|\ \nu(\omega) \quad (36)$$

to give Eq. (8). The simplicity of this result is due to the fact that Q and G have the same symmetry properties. If we have a concentration D of defects with a refractive index n then finally (following say Ref. 10)

$$K(\omega) = \frac{2\pi^2 ND\alpha^2}{nc}\left(\frac{\omega}{\omega_{\mathrm{cell}}}\right)^4\ |\chi^2(0,\omega^2)|\ \nu(\omega). \quad (37)$$

IV. CALCULATION FOR FACE-CENTERED CUBIC LATTICE

The normalized fourfold basis of the F_{1u} mode is given for the fcc lattice as[11]

$$\begin{aligned}
\alpha_0 &= u_x(0,0,0),\\
2\sqrt{2}\alpha_1 &= u_x(1,1,0) + u_x(\bar1,\bar1,0) + u_x(1,0,1)\\
&\quad + u_x(\bar1,0,\bar1) + u_x(1,\bar1,0) + u_x(\bar1,1,0)\\
&\quad + u_x(\bar1,0,1) + u_x(1,0,\bar1),\\
2\sqrt{2}\alpha_2 &= u_y(1,1,0) + u_y(\bar1,\bar1,0) + u_z(1,0,1) + u_z(\bar1,0,\bar1)\\
&\quad - u_y(1,1,0) - u_y(\bar1,1,0) - u_z(\bar1,0,1) - u_z(1,0,\bar1),\\
2\alpha_3 &= u_x(0,1,1) + u_x(0,\bar1,\bar1) + u_x(0,1,\bar1) + u_x(0,\bar1,1). \quad (38)
\end{aligned}$$

We define

$$\begin{aligned}
&g_0 = g_{xx}(000), \quad g_1 = g_{xx}(110),\\
&g_2 = g_{xy}(110), \quad g_3 = g_{xx}(011),\\
&A = g_0 + g_{xx}(020) + g_{xx}(200) + g_{xx}(220),\\
&B = g_{xy}(220) + 2g_{xy}(211),\\
&D = g_{xx}(200) + g_{xx}(020) - g_{xx}(220) - g_0,\\
&F = g_0 + 2g_{xx}(020) + g_{xx}(022), \quad (39)\\
&C' = g_3 + g_{xx}(211),\\
&E' = g_{xy}(112) - g_2,\\
&H = g_1 + g_{xx}(121),\\
&K = g_{xy}(211).
\end{aligned}$$

Thus in the normalized basis $(\alpha_0, \alpha_1, \alpha_2, \alpha_3)$ the matrix of G_0 is

$$[G_0]_{F_{1u}} = \begin{pmatrix} g_0 & 2\sqrt{2}g_1 & 2\sqrt{2}g_2 & 2g_3 \\ 2\sqrt{2}g_1 & A+2C' & B & 2\sqrt{2}H \\ 2\sqrt{2}g_2 & B & 2E'-D & 2\sqrt{2}K \\ 2g_3 & 2\sqrt{2}H & 2\sqrt{2}K & F \end{pmatrix} \quad (40)$$

and the matrix of V is

$$[V]_{F_{1u}} = \begin{pmatrix} V_{xx}(00) & 2\sqrt{2}\,V_{xx}(110) & 2\sqrt{2}\,V_{xy}(110) & 2V_{xx}(011) \\ 2\sqrt{2}\,V_{xx}(110) & -V_{xx}(110) & -V_{xy}(110) & 0 \\ 2\sqrt{2}\,V_{xy}(110) & -V_{xy}(110) & -V_{xx}(110) & 0 \\ 2V_{xx}(011) & 0 & 0 & -V_{xx}(011) \end{pmatrix}. \quad (41)$$

In the nearest-neighbor approximation the Green's-function relations are

$$\begin{aligned}
&A_{xx}(00)g_0 + 8A_{xx}(110)g_1 + 8A_{xy}(110)g_2 + 4A_{xx}(011)g_3 = 1 + M\omega^2 g_0,\\
&A_{xx}(00)g_1 + A_{xx}(110)(A+2C') + A_{xy}(110)B + 2A_{xx}(011)H = M\omega^2 g_1,\\
&A_{xx}(00)g_2 + A_{xx}(110)B + A_{xy}(110)(2E'-D) + 2A_{xx}(011)K = M\omega^2 g_2,\\
&A_{xx}(00)g_3 + 4A_{xx}(110)H + 4A_{xy}(110)K + A_{xx}(011)F = M\omega^2 g_3. \quad (42)
\end{aligned}$$

The quantities H, C', E' are different from those used in Ref. 1 and the above equations are slightly altered compared to their previous form. Also the matrix G_0V does not coincide with that given by reading off from Eqs. (23) of Ref. 1. None of the final conclusions of Ref. 1 are altered by these errors, which were only due to carelessness by one of us when he prepared the earlier paper. We make the central-force approximation as before, so that

$$\begin{aligned}
&8V_{xx}(110) = 8V_{xy}(110) = -\epsilon M\omega^2 - V_{xx}(00),\\
&V_{xx}(011) = 0,\\
&8A_{xx}(110) = 8A_{xy}(110) = -A_{xx}(00),\\
&A_{xx}(011) = 0. \quad (43)
\end{aligned}$$

The external perturbation is given by

$$Q = \frac{\alpha^2}{8}\begin{pmatrix} 8 & -2\sqrt{2} & -2\sqrt{2} & 0 \\ -2\sqrt{2} & 1 & 1 & 0 \\ -2\sqrt{2} & 1 & 1 & 0 \\ 0 & 0 & 0 & 0 \end{pmatrix}, \quad (44)$$

and the inverse matrix is given by

$$\Delta(1-G_0V)^{-1}=\begin{pmatrix} 1+\lambda M\omega^2(g_1+g_2), & -\frac{\lambda}{2\sqrt{2}}(1+M\omega^2 g_0), & -\frac{\lambda}{2\sqrt{2}}(1+M\omega^2 g_0), & 0 \\ -2\sqrt{2}M\omega^2(\epsilon-\lambda)g_1, & 1-\lambda+M\omega^2(\epsilon-\lambda)g_0, & -\lambda M\omega^2(1-\epsilon)g_1, & 0 \\ & +\lambda M\omega^2(1-\epsilon)g_2 & & \\ -2\sqrt{2}M\omega^2(\epsilon-\lambda)g_2, & -\lambda M\omega^2(1-\epsilon)g_2, & 1-\lambda+M\omega^2(\epsilon-\lambda)g_0, & 0 \\ & & +\lambda M\omega^2(1-\epsilon)g_1 & \\ -2M\omega^2(\epsilon-\lambda)g_3, & -\frac{\lambda M\omega^2}{\sqrt{2}}(1-\epsilon)g_3, & -\frac{\lambda M\omega^2}{\sqrt{2}}(1-\epsilon)g_3, & \Delta \end{pmatrix}. \quad (45)$$

Then on calculation we again obtain all the previous results as in the bcc case, which follows since the fcc is its reciprocal lattice.

V. APPLICATION TO IMPURITY-INDUCED ABSORPTION SPECTRA

Some years ago Jones and Woodfine[12] made an experimental study of the far-ir absorption spectra of xenon and krypton impurities in solid argon. Their experimental data are presented in Fig. 1. The most interesting feature of their measurements was that the observed spectrum of xenon in argon resembled closely a phonon spectrum for pure solid argon calculated theoretically by Grindlay and Howard[13] using a Lennard-Jones potential model. There have since been various attempts[5,6,10] to fit the experimental data, all of which involved either unclear approximations or detailed numerical work. Though the fits were satisfactory enough, the nature of the approximations employed make it difficult to say what has been learned by them. Having reduced the problem to our simple formula of Eq. (8), we shall now apply it to the data to obtain a clearer physical picture of what is happening. However, in order to do this, we need a phonon spectrum for the pure crystal, so we first discuss what is known theoretically and experimentally about the density of states of solid argon.

On the experimental side there has been a study by Randolph[14] using inelastic neutron scattering. This experiment was performed just below the melting point at 80 °K and yielded a spectrum similar to that of Ref. 13 with its characteristic transverse and longitudinal mode maxima. The experimental cutoff was found to be $\omega_{max}=64$ cm^{-1}. The calculation of Ref. 13 was a 0 °K calculation giving a cutoff of 68.1 cm^{-1}. In it the two parameters σ and ϵ of the Lennard-Jones potential were determined from 0 °K measurements of the lattice spacing, some elasticity constants, and the Debye frequency ω_D. The values obtained for σ and ϵ were then found to coincide with their gas-phase values. Also at 0 °K the experimental ω_D is found to be 64.8 cm^{-1} after extrapolation.[15] Since the Debye model replaces the Brillouin zone by a sphere of the same volume it must give $\omega_D < \omega_{max}$. Further, as we go to higher temperatures the lattice expands bringing about a reduction in forces and hence in frequencies. Thus both the specific-heat and neutron-scattering data support the slightly higher theoretical value for the 0 °K cutoff. There is also some further indirect evidence for this value. Recently Mannheim and Friedmann[16] have developed a theory of the far-ir absorption spectra of diatomic molecules embedded in rare-gas crystals. Using this theory they were able to identify localized modes seen in various experimental spectra and calculate their positions. The localized modes were found to be very close to the band edge and their positions very sensitive to the value of ω_{max}. [This follows since $\rho(\omega^2)$ of Eq. (2) depends directly on ω^2_{max}.] Hence this analysis confirms the above value of ω_{max}, and we shall use it below in this work.

Rather than use the somewhat old spectrum of Grindlay and Howard, we have recalculated the density of states using a method developed by Gilat and

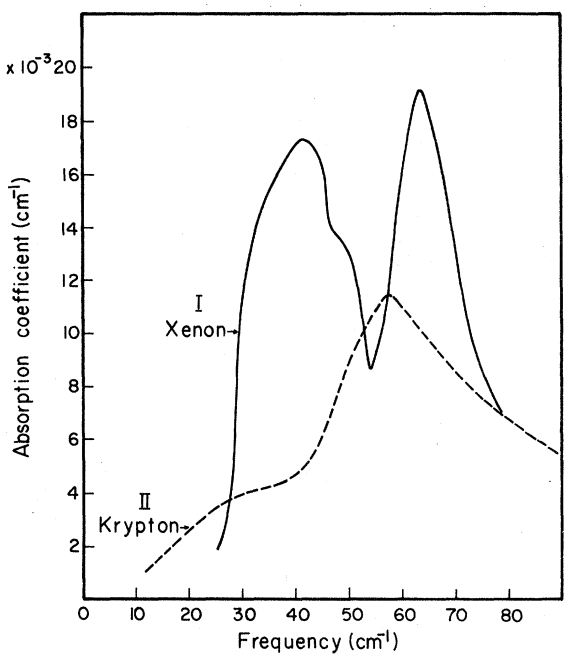

FIG. 1. Curves I and II show the experimental data taken from Ref. 12. Curve I refers to the far-ir impurity induced absorption spectrum of $\frac{1}{2}$% xenon in solid argon at 55 °K, while curve II refers to 1% krypton impurities in solid argon at 80 °K. The frequency w is plotted in wave numbers.

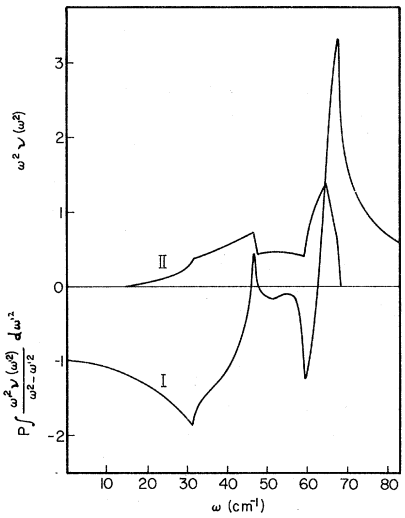

FIG. 2. Curve I is a plot of the function $S(\omega^2)$ using our calculated density of states for solid argon. Curve II shows $\omega^2\nu(\omega^2)$ as a function of the frequency ω, and reflects the characteristic transverse- and longitudinal-mode maxima of $\nu(\omega)$. In both curves $\nu(\omega^2)$ is normalized to unity.

Raubenheimer.[17] We use the same Lennard-Jones model with the same parameters as in Ref. 13. Naturally the two calculations yield similar spectra, but since we take more points in the Brillouin zone and use a more refined technique, we have a smoother and more accurate $\nu(\omega)$. We present our calculated density of states in Fig. 2 by plotting the convenient function $\omega^2\nu(\omega^2)$ using the normalization $\int\nu(\omega^2)d\omega^2=1$. For reference purposes we have also plotted the function $S(\omega^2)$ of Eq. (3) as calculated from our density of states.

In order to apply Eq. (8) to the experimental data of Ref. 12 we also need to know the changed force ratio λ. To get an estimate we have used a Lennard-Jones model with the empirical combining

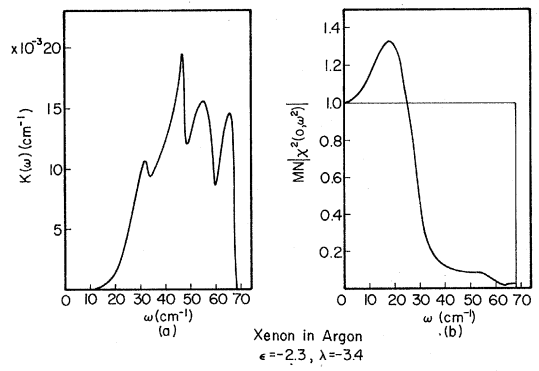

FIG. 3. (a) Plot of $K(\omega)$; (b) plot of $MN|\chi^2(0,\omega^2)|$, both graphs as a function of ω. Graph (a) is scaled to the experimental data of Ref. 12. The computed values refer to the case of xenon in argon with $\epsilon=-2.3$ and $\lambda=-3.4$.

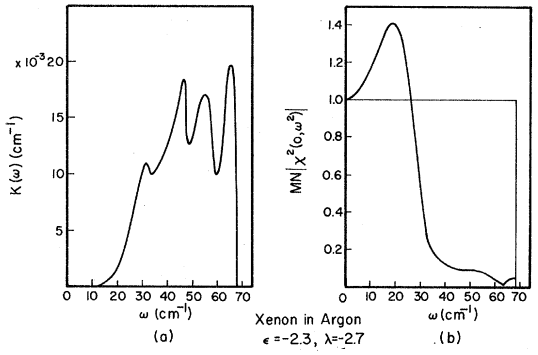

FIG. 4. $MN|\chi^2(0,\omega^2)|$ and $K(\omega)$ for the case of xenon in argon with $\epsilon=-2.3$ and $\lambda=-2.7$.

laws $\sigma_{12}=\frac{1}{2}(\sigma_1+\sigma_2)$, $\epsilon_{12}=(\epsilon_1\epsilon_2)^{1/2}$. This model was reasonably successful when applied in Ref. 16. The model then gives $\lambda=-0.9$ for krypton in argon and $\lambda=-3.4$ for xenon in argon. The mass ratios we use are $\epsilon=-1.1$ and $\epsilon=-2.3$, respectively, in the two cases. As well as use the above values of λ, we have also treated λ as a free parameter to be varied, and our best fits are then obtained with the values $\lambda=-0.2$ for krypton in argon and $\lambda=-2.7$ for xenon in argon. In Figs. 3–6 we have plotted the amplitude $MN|\chi^2(0,\omega^2)|$ and the absorption coefficient $K(\omega)$ for all the above cases. We have not made any attempt to determine the scale of $K(\omega)$ as we do not have any suitable model for the effective charge α^2 and have only studied the shape of the spectra. Our calculations strictly apply only at 0 °K, whereas the experiments were performed at 55 °K for xenon impurities and at 80 °K for krypton impurities. As we noted above, at these higher temperatures ω_{max} is reduced somewhat, so our curves should be squeezed a fraction to lower frequencies before making a comparison. We do not attach too much significance to our model estimates for λ, and note only that they give the same order of magnitude and sign as our best-fit values. We found that we could obtain equally satisfactory fits for a range of λ's around the above quoted ones, as

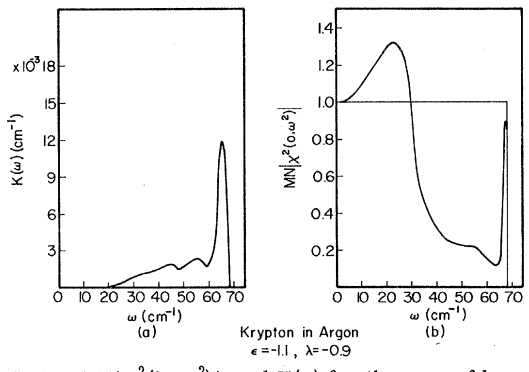

FIG. 5. $MN|\chi^2(0,\omega^2)|$ and $K(\omega)$ for the case of krypton in argon with $\epsilon=-1.1$ and $\lambda=-0.9$.

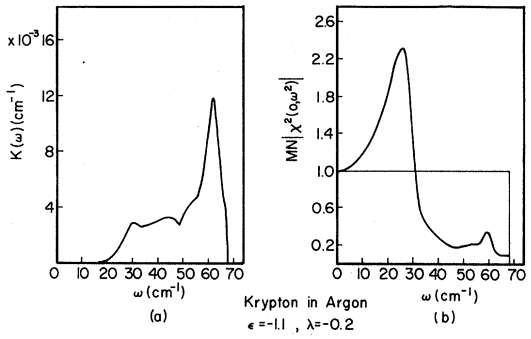

FIG. 6. $MN|\chi^2(0,\omega^2)|$ and $K(\omega)$ for the case of krypton in argon with $\epsilon=-1.1$ and $\lambda=-0.2$.

the raw data are rather rough.

We regard the fitting for xenon as reasonable and that for krypton as more than good. As we have calculated $|\chi^2(0,\omega^2)|$ we can see clearly the modulating effect that the defect motion has on the absorption spectrum. For the krypton fitting with $\lambda=-0.2$ we see that $|\chi^2(0,\omega^2)|$ has a peak just below the longitudinal-mode maximum and this is then emphasized in $K(\omega)$. At first sight it appears that this must be a resonance mode. However, we find that the peak frequency does *not* solve Eq. (6) even approximately. As we have discussed in Ref. 1 not all the maxima in $|\chi^2(0,\omega^2)|$ need be resonance modes, since some of them are fixed simply by the approximate vanishing of $d|\chi^2(0,\omega^2)|/d\omega^2$, which is presumably the case here. For the xenon fitting with $\lambda=-2.7$ we see that $|\chi^2(0,\omega^2)|$ takes appreciable values for low frequencies, but is quite small near the longitudinal-mode maximum. However, there is an additional frequency-dependent factor $(\omega/\omega_{\text{cell}})^4$ in $K(\omega)$, and this then emphasizes the high-frequency part of the spectrum. Thus finally we obtain an absorption spectrum similar in shape to the density of states of the pure crystal, but we see that this is just a coincidence. The reason that $|\chi^2(0,\omega^2)|$ falls off for the high-frequency band modes is because for xenon in argon there is also a localized mode near the band edge which takes some intensity out of the band modes. We discuss now why this localized mode is not visible in the spectrum.

To determine the intensity in a localized mode we can either use Eq. (7b) directly, or appeal to the normalization condition[2]

$$M'\int_0^\infty|\chi^2(0,\omega^2)|\,\nu(\omega^2)\,d\omega^2=1. \tag{46}$$

The integration includes both band modes and localized modes as well, so that

$$M'|\chi^2(0,\omega_L^2)|=1-M'\int_0^{\omega_{\max}}|\chi^2(0,\omega^2)|\,\nu(\omega^2)\,d\omega^2. \tag{47}$$

If we insert the two parts of Eq. (7) on either side of Eq. (47) we of course have an identity. However, the resulting relation is by no means obvious, and has been justified independently by Dawber and Elliott[3] using complex-variable techniques. Thus using both Eqs. (7) and (47) provides a check on the accuracy of the numerical integrations involved in determining $|\chi^2(0,\omega^2)|$. For the case of interest, i.e., xenon in argon with $\lambda=-2.7$, we find that $\omega_L=76\ \text{cm}^{-1}$ with $M'|\chi^2(0,\omega_L^2)|=0.27$. This should be compared to the case of HCl in argon ($\epsilon=0.1$, $\lambda=-0.9$), where there is a localized mode in the same position with $M'|\chi^2(0,\omega_L^2)|=0.7$.[16] As noted in Ref. 16, for the case of HCl in argon the longitudinal-mode maximum is completely eliminated from $K(\omega)$, but for xenon in argon we see that the localized mode has much less of the intensity which goes mainly into the band modes.

Apart from the intensity, the other factor which determines whether or not the localized mode may be picked up in the absorption spectrum is its width. The mode may acquire a width due to anharmonic forces, i.e.,[16]

$$\Gamma(\omega_L)\sim\sum_{\substack{\alpha,\beta,\gamma,l_2,l_3\\ \omega_2,\omega_3}}|A_{\alpha\beta\gamma}(0,l_2,l_3)|^2\times|\chi_\alpha(0,\omega_L^2)|^2\,|\chi_\beta(l_2,\omega_2^2)|^2\,|\chi_\gamma(l_3,\omega_3^2)|^2\times\delta(\omega_L-\omega_2-\omega_3)\,\nu(\omega_2)\,\nu(\omega_3), \tag{48}$$

where we have only retained the cubic anharmonic contribution. For HCl in argon the typically reported anharmonic widths were of the order of 10 cm^{-1}. We note that the width depends not on $M'|\chi^2(0,\omega_L^2)|$, but only on $|\chi^2(0,\omega_L^2)|$, so that we may safely expect an anharmonic width for xenon in argon of less than 1 cm^{-1}. This of course is too small to be observable in the experiment of Ref. 12 which used a 5-cm^{-1} spectral slit width, and we suspect that the localized mode lies buried under the high-frequency multiphonon tail of Fig. 1.

VI. GENERAL DISCUSSION OF THE WORK

In this work we have shown how to exploit the high local symmetry at defect sites so as to include force-constant changes. The closed expressions we have provided are simple and allow for the inclusion of force changes without any need to use perturbation approximations. In particular our results for xenon in argon show specifically the influence of force changes even in the presence of a large mass change, since if we were only to consider the large mass increase we would not anticipate the presence of localized modes at all. Further, the force change has a marked effect in $|\chi^2(0,\omega^2)|$, the modulating factor in the absorption coefficient. Though we have referred specifically to optical absorption, our analysis of the response function is general and may be applied in neutron-scattering or one-phonon Mössbauer experiments as well.

Dawber and Elliott[18] have made a study of the absorption due to a point charge in a crystal, where the absorption coefficient is given by

$$K(\omega) \sim N \left| \chi^2(0, \omega^2) \right| \nu(\omega). \tag{49}$$

This should be contrasted with our Eq. (8) which has an additional $(\omega/\omega_{cell})^4$ factor. There is of course no connection between the two calculations as they correspond to different physical situations. In the present case of absorption due to an induced dipole we have to consider the composite system of the defect and its neighbors whose total electric charge is zero. Though Eqs. (6) and (7) reduce to the standard mass-defect equations in the limit $\lambda \to 0$, we note that in the present absorption case if there were no force change there would be no effective charge and hence no absorption at all. Further, from Newton's third law of motion it is not possible to change the force at the defect site without making a compensating change at the neighbor sites. Thus we have to take into account the motion of the neighbors as well from the very beginning, and this is why the absorption is normalized to the cell-model limit. It is generally supposed that the cell model is only valid in the asymptotic limit, i.e., $\omega_{cell} \gg \omega_{max}$. However, its range of applicability is in fact much greater, and under certain conditions it may even be valid near the band edge.[19] Thus the maximum optical response is given when the defect is moving with the most-favored frequency supplied by its neighbors, i.e., the cell frequency.

A situation in which we do put a charge directly into the crystal may be realized by taking nonsymmetrical diatomic molecules (such as HCl) as defects. The physical mechanism responsible for the absorption rotation-translation coupling is discussed in detail in Ref. 16. This coupling mechanism is between the internal degrees of rotation of the diatomic molecule and the translational motion of its center of charge in the cell potential of the neighbors, i.e., coupling between the rotation and the phonon states. The absorption coefficient determined in Ref. 16 is

$$K(\omega) \sim M'^2 N \left| \chi^2(0, \omega^2) \right| \omega^6 \left(\frac{1}{\hbar\omega - 2B} + \frac{1}{\hbar\omega + 2B} \right)^2 \nu(\omega), \tag{50}$$

where B is the rotational constant of the molecule. Thus in the limit $\hbar\omega \gg 2B$ we again obtain an ω^4 factor.

To conclude we would like to express the opinion that Eqs. (8) and (50) provide us with a quite powerful way of obtaining information about the density of states of pure crystals. By choosing a variety of probes it should be possible to isolate the critical points in the phonon spectra. One particularly amusing proposal is to use H_2 and HD as defects. The force changes are the same in the two cases, but the absorption mechanisms are completely different. H_2 will give an induced-dipole-moment spectrum [Eq. (8)], whereas HD will give the permanent-dipole-moment spectrum of Eq. (50), and yet the only differences (apart from the over-all scale) will be due to the known HD rotational constant.

ACKNOWLEDGMENTS

One of us (S. S. C.) would like to thank Professor S. Kimel and Dr. A. Ron for useful discussions. He is also indebted to Professor Abdus Salam, Professor Paolo Budini, and Professor Stig Lundqvist for their hospitality at the International Center for Theoretical Physics, Trieste, where part of this work was carried out. The other one of us (P. D. M.) would like to thank Professor Y. Ne'eman for the hospitality of the Department of Physics and Astronomy at Tel-Aviv University while this work was in its initial stages, and also would like to thank Professor I. Prigogine for the hospitality of the Faculté des Sciences at Université Libre de Bruxelles.

*Research sponsored in part by Les Instituts Internationaux de Physique et Chimie fondés par E. Solvay.

[1]P. D. Mannheim, Phys. Rev. 165, 1011 (1968).

[2]A. A. Maradudin, Rept. Progr. Phys. 28, 331 (1965); A. A. Maradudin, in *Solid State Physics*, edited by F. Seitz and D. Turnbull (Academic, New York, 1966), Vols. 18 and 19.

[3]P. G. Dawber and R. J. Elliott, Proc. Roy. Soc. (London) A273, 222 (1963).

[4]G. W. Lehman and R. W. De Wames, Phys. Rev. 131, 1008 (1963).

[5]T. P. Martin, Phys. Rev. 160, 686 (1967).

[6]W. M. Hartmann and R. J. Elliott, Proc. Phys. Soc. (London) 91, 187 (1967).

[7]This relation is also provided in Ref. 8 [Eq. (7) of that reference] where unfortunately there was a typing error.

[8]P. D. Mannheim and A. Simopoulos, Phys. Rev. 165, 845 (1968).

[9]M. Born and K. Huang, *Dynamical Theory of Crystal Lattices* (Oxford U.P., New York, 1954).

[10]R. O. Davies and D. Healey, Proc. Phys. Soc. (London) C1, 1184 (1968).

[11]K. Dettmann and W. Ludwig, Physik Kondensierten Materie 2, 241 (1964).

[12]G. O. Jones and J. M. Woodfine, Proc. Phys. Soc. (London) 86, 101 (1965).

[13]J. Grindlay and R. Howard, in *Proceedings of the International Conference on Lattice Dynamics, Copenhagen*, 1963, edited by R. F. Wallis (Pergamon, New York, 1965), p. 129.

[14]P. D. Randolph, Phillips Petroleum Co. Report No. IDO 17089, 1965 (unpublished).

[15]G. L. Pollack, Rev. Mod. Phys. 36, 748 (1964).

[16]P. D. Mannheim and H. Friedmann, Phys. Status Solidi 39, 409 (1970).

[17]G. Gilat and L. J. Raubenheimer, Phys. Rev. 144, 390 (1966).

[18]P. G. Dawber and R. J. Elliott, Proc. Phys. Soc. (London) 81, 453 (1963).

[19]P. D. Mannheim, Phys. Rev. (to be published).